Multiple optomechanically induced transparency in the hybrid optomechanical system with the two-level and three-level atomic ensembles

Gongtao Yu(余功涛)[1,2,3], Guixia Pan(潘桂侠)[5], Yongyang Yu(于永洋)[1,2,3], Junliang Jiang(江俊良)[1,2,3], Wenqu Xu(许问渠)[1,2,3], Kaixuan Zhang(张凯旋)[1,2,3], Quan Zuo(左权)[1,2,3], Tianshi Zhou(周天石)[1,2,3], Tingting Guo(郭婷婷)[1,2,3], Mingyuan Yu(俞铭远)[1,2,3], Chunhai Cao(曹春海)[1,3], Guozhu Sun(孙国柱)[1,2,3,4,†], and Peiheng Wu(吴培亨)[1,2,3]

[1] *Research Institute of Superconductor Electronics, School of Electronic Science and Engineering, Nanjing University, Nanjing* 210023, *China*
[2] *Purple Mountain Laboratories, Nanjing* 211111, *China*
[3] *Hefei National Laboratory, Hefei* 230088, *China*
[4] *Shishan Laboratory, Suzhou Campus of Nanjing University, Suzhou* 215163, *China*
[5] *School of Mechanics and Optoelectronic Physics, Anhui University of Science and Technology, Huainan* 232001, *China*

(Received 26 November 2025; revised manuscript received 15 January 2026; accepted manuscript online 6 February 2026)

We investigate the optomechanically induced transparency in a hybrid optomechanical system, which consists of two optical cavities and a mechanical resonator. The two-level and three-level atomic ensembles are trapped in the two optical cavities, respectively. We focus on the changes in the number and width of transparency windows and the position of transparent points under different conditions influenced by various interactions. Five transparency windows can be observed when all the interactions are on. The introduction of two-level and three-level atomic ensembles can increase the number of transparency windows and also provide better flexibility for controlling the width of the transparency windows. Specifically, the two-level and three-level atomic ensembles contribute one and two transparency windows, respectively. The stronger coupling results in the larger transparency windows and movement of the transparent points. Moreover, we also study the slow/fast light phenomenon through the variation of phase and group delay. These results may contribute to the research of nonlinear optics and have potential applications in optical signal processing and communication.

Keywords: optomechanically induced transparency, optomechanical system, atomic ensemble

PACS: 42.50.pq, 03.67.–a, 42.50.Ex

DOI: 10.1088/1674-1056/ae42b8 **CSTR:** 32038.14.CPB.ae42b8

1. Introduction

Optomechanics[1–22] describes the coupling between the optical degree of freedom and the mechanical one through the radiation pressure interaction. Its rapid development provides a broader scope for research in quantum physics. Recently, a series of intriguing optical phenomena have been intensively explored in the cavity optomechanical system such as phonon squeezing,[23] slow and fast light,[24] Kerr effect,[25] normal mode splitting,[26] and signal amplification.[27] Optomechanically induced transparency (OMIT) is a phenomenon similar to electromagnetically induced transparency, arising from the interference cancellation of different paths in the optomechanical system. The OMIT effect plays a crucial role in quantum technology and has a rich variety of applications, including steady-state entanglement,[28] quantum sensing,[29] single-photon routers,[30] signal processing,[31] quantum ground state cooling,[32] controlled photon propagation,[33] and charge measurement.[34]

Double-OMIT[35–42] has been intensively studied in the cavity optomechanical system. Jiang *et al.*[35] proposed a model in which N mechanical modes were coupled to a common optical mode. They systematically demonstrated the mechanism of double-transparency windows and found that adjusting the amplitude and phase of the external field could affect the absorption of the probe field. This laid the foundation for the following research. Subsequently, more diverse physical platforms and coupling mechanisms have been explored. For example, some researchers extended the coupling mechanism to the parity-time-symmetric optomechanical system.[36] By calculating the transmission rate of the probe field, they specifically analyzed the influence of Coulomb coupling on the double optomechanical induced absorption. More interestingly, some researchers investigated the tunable optomechanical induced transparency phenomenon in a new three-mode ring coupling system.[38,39] They achieved the double-OMIT phenomenon by introducing phonon exchange interactions related to the phase. By introducing multiple coupled fields or atoms, multiple-OMIT[43–48] are generated on the optical response spectrum, significantly enhancing the control ability over the propagation behavior of light. For instance, Xiao *et al.*[43] theoretically investigated the OMIT

†Corresponding author. E-mail: gzsun@nju.edu.cn

© 2026 Chinese Physical Society and IOP Publishing Ltd. All rights, including for text and data mining, AI training, and similar technologies, are reserved.

CPB Online in Press

phenomenon in the single-cavity optomechanical system and N-cavity optomechanical system. The results showed that the output field of the system could have at most N transparency windows. Furthermore, the coupling between atoms and cavity fields also provides a new way for the formation of multiple-OMIT. For an N-cavity optomechanical system that is doped with a pair of Rydberg atoms, the coupling between the two Rydberg atoms and cavity field will result in the appearance of two additional transparency windows.[44] The alteration of the quantum interference path will also have an impact on the OMIT. Furthermore, the cavity optomechanical system acting on the pump field and probe field of different cavities provides a new method for generating multiple-OMIT.[45]

The introduction of the atomic ensemble into optical cavities leads to many nonlinear effects and related applications such as quantum entanglement,[49] single photon emission,[50] quantum chaos,[51] cavity subradiance and superradiance,[52] and cavity sideband cooling.[53] However, the OMIT phenomenon in the hybrid cavity optomechanical system containing two different types of atomic ensembles has not received much attention. The effect of atomic media will enrich the characteristics of the system.

Here in our system, the two-level atomic ensemble is trapped in the optical cavity a_1, while the three-level atomic ensemble is trapped in the optical cavity a_2. In contrast to previous studies,[54,55] our model incorporates both the two-level and three-level atomic ensembles into the system simultaneously. The increased coupling effect leads to more transparency windows appearing in the output spectrum and provides more possibilities for effectively regulating the OMIT phenomenon. In addition, two optical microcavities are coupled to each other through the common waveguide and the optical cavity a_2 is coupled to a mechanical resonator b_1 under the radiation pressure. Different interactions within the system on OMIT lead to the changes in the number and width of transparency windows and also change the position of transparent points. These interactions include the action of the two-level atomic ensemble on the cavity field a_1, the action of the three-level atomic ensemble on the cavity field a_2, the coupling between the two optical cavities, and the coupling between the optical and mechanical modes.

2. Model and solutions

As depicted in Fig. 1, we consider an optomechanical system consisting of two optical cavities (a_1, a_2) and a mechanical resonator (b_1). The optical cavity a_1 with frequency ω_1 and the optical cavity a_2 with frequency ω_2 are coupled via a distant waveguide with hopping rate J. Meanwhile, the two-level atomic ensemble is trapped inside a_1 and the Λ-type three-level atomic ensemble is trapped inside a_2. The nanomechanical resonator b_1 with frequency $\omega_{\rm m1}$ is coupled to a_2 via radiation pressure. a_1 is coherently driven by a strong control field $\varepsilon_{\rm c}$ with frequency $\omega_{\rm c}$ and a weak probe field $\varepsilon_{\rm p}$ with frequency $\omega_{\rm p}$.

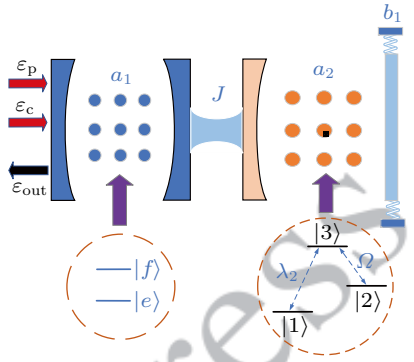


Fig. 1. Schematic diagram of the cavity optomechanical system. It includes two cavities a_1 and a_2 with the interactive coupling strength J and a mechanical resonator b_1 coupling to a_2 with the coefficient g. The two-level and three-level atomic ensembles are placed inside two cavities, respectively.

In the rotating frame at the frequency $\omega_{\rm c}$, the Hamiltonian of the system is described as[36,44,56,57]

$$\begin{aligned}
H &= H_0 + H_{\rm int} + H_{\rm dr},\\
H_0 &= \hbar\Delta_1 a_1^\dagger a_1 + \hbar\Delta_2 a_2^\dagger a_2 + \hbar\omega_{\rm m1} b_1^\dagger b_1\\
&\quad + \hbar\sum_{n=1}^{N}\omega_{fe}\sigma_{ff}^{(n)} + \hbar\sum_{i=1}^{N}E_{21}\sigma_{22}^{(i)} + E_{31}\sigma_{33}^{(i)},\\
H_{\rm int} &= \hbar J(a_1^\dagger a_2 + a_2^\dagger a_1) + \hbar g a_2^\dagger a_2(b_1^\dagger + b_1)\\
&\quad + \hbar\lambda_1\sum_{n=1}^{N}(a_1\sigma_{fe}^{(n)} + a_1^\dagger\sigma_{ef}^{(n)})\\
&\quad + \hbar\lambda_2\sum_{i=1}^{N}(a_2^\dagger\sigma_{13}^{(i)} + a_2\sigma_{31}^{(i)})\\
&\quad + \hbar\Omega\sum_{i=1}^{N}(\mathrm{e}^{-\mathrm{i}\omega_{\rm c}t}\sigma_{32}^{(i)} + \mathrm{e}^{\mathrm{i}\omega_{\rm c}t}\sigma_{23}^{(i)}),\\
H_{\rm dr} &= \mathrm{i}\hbar\varepsilon_{\rm c}(a_1^\dagger - a_1) + \mathrm{i}\hbar\varepsilon_{\rm p}(a_1^\dagger\mathrm{e}^{-\mathrm{i}\Delta_{\rm p}t} - a_1\mathrm{e}^{\mathrm{i}\Delta_{\rm p}t}). \qquad (1)
\end{aligned}$$

Here H_0 is the free Hamiltonian of the optomechanical system, which includes the two cavities, mechanical resonator, two-level and Λ-type three-level atomic ensembles. Here, a_j $(a_j^\dagger, j = 1,2)$ and b_1 $(b_1^\dagger)$ are the annihilation (creation) operators.[58] $\Delta_1 = \omega_1 - \omega_{\rm c}$ and $\Delta_2 = \omega_2 - \omega_{\rm c}$ represent the frequency detunings between the control field and the two cavity fields. $\sigma_{\alpha\alpha'}^{(i)} = |\alpha\rangle^{(i)}\langle\alpha|\,(\alpha,\alpha' = e,f)$ is the spin operator of the atom, $|e\rangle$ and $|f\rangle$ are the ground and excited states of the two-level ensemble, respectively. The frequency ω_{fe} represents the energy level spacing between $|e\rangle$ and $|f\rangle$. The different energy levels within the three-level atomic ensemble can be represented as $|1\rangle$, $|2\rangle$, and $|3\rangle$ with the corresponding atom spin operator $\sigma_{\beta\beta'}^{(i)} = |\beta\rangle^{(i)}\langle\beta|$ $(\beta,\beta' = 1,2,3)$. The frequencies E_{21} and E_{31} represent the energy level spacing between the different energy levels. $H_{\rm int}$ describes the interaction Hamiltonian, in which the first line shows the coupling energy between two distant cavities and the interaction energy between the optical and mechanical modes. The next two lines

CPB Online In-press

represent the interaction energies between the two atomic ensembles and the two cavity fields with the corresponding coupling coefficients λ_1 and λ_2. The last line represents the interaction between the atomic ensemble and the classical laser field with the coupling strength Ω. $H_{\rm dr}$ is the driving term of two external light fields. The amplitude of the control (probe) field is $\varepsilon_{\rm c}=\sqrt{\frac{2\kappa_1 P_{\rm c}}{\hbar\omega_{\rm c}}}$ $\left(\varepsilon_{\rm p}=\sqrt{\frac{2\kappa_1 P_{\rm p}}{\hbar\omega_{\rm p}}}\right)$ with the corresponding power $P_{\rm c}$ ($P_{\rm p}$). $\Delta_{\rm p}=\omega_{\rm p}-\omega_{\rm c}$ is the detuning between the probe and pump fields.

Under the condition that the number of atoms is very large and in a low excited state, the atomic ensemble can be considered as a whole and represented by the collective atom operator. We assume that the collective quasi-spin operator of the two-level atomic ensemble is $A=\frac{1}{\sqrt{N}}\sum_{n=1}^{N}\sigma_{ef}^{(n)}$, and the collective quasi-spin operators of the three-level atomic ensemble are $B_1=\frac{1}{\sqrt{N}}\sum_{i=1}^{N}\sigma_{13}^{(i)}$ and $B_2=\frac{1}{\sqrt{N}}\sum_{i=1}^{N}\sigma_{12}^{(i)}$. They satisfy the bosonic commutation relations $[A,A^{\dagger}]=1$, $[B_1,B_1{}^{\dagger}]=1$, and $[B_2,B_2{}^{\dagger}]=1$.

Considering the dissipation and fluctuation terms of the optomechanical system, we get the quantum Langevin equations

$$\begin{aligned}
\dot{a}_1 &= -(\kappa_1+{\rm i}\Delta_1)a_1-{\rm i}Ja_2-{\rm i}G_A A\\
&\quad+\varepsilon_{\rm c}+\varepsilon_{\rm p}\,{\rm e}^{-{\rm i}\Delta_{\rm p}t}+f_{a_1},\\
\dot{a}_2 &= -(\kappa_2+{\rm i}\Delta_2)a_2-{\rm i}Ja_1-{\rm i}ga_2(b_1^{\dagger}+b_1)\\
&\quad-{\rm i}G_B B_1+f_{a_2},\\
\dot{b}_1 &= -(\gamma_{\rm m1}+{\rm i}\omega_{\rm m1})b_1-{\rm i}ga_2^{\dagger}a_2+f_{b_1},\\
\dot{A} &= -(\gamma_A+{\rm i}\Delta_A)A-{\rm i}G_A a_1+f_A,\\
\dot{B}_1 &= -(\gamma_{B_1}+{\rm i}\Delta_B)B_1-{\rm i}G_B a_2-{\rm i}\Omega B_2+f_{B_1},\\
\dot{B}_2 &= -(\gamma_{B_2}+{\rm i}E_{21})B_2-{\rm i}\Omega B_1+f_{B_2},
\end{aligned}\tag{2}$$

where $G_A=\lambda_1\sqrt{N}$ and $G_B=\lambda_2\sqrt{N}$. $\Delta_A=\omega_{fe}-\omega_{\rm c}$ and $\Delta_B=\omega_{31}-\omega_{\rm c}$ are the detunings. κ_1, κ_2, $\gamma_{\rm m1}$, γ_A, γ_{B_1}, and γ_{B_2} are the decay rates of the two optical modes, mechanical mode, and atoms, respectively. f_{a_1}, f_{a_2}, f_{b_1}, f_A, f_{B_1}, and f_{B_2} are the corresponding environmental noises,[26,36,59] which satisfy the condition $\langle f(t)\rangle=0$.

In the case of $\varepsilon_{\rm c}\gg\varepsilon_{\rm p}$, we assume the dynamical variables as the sum of their steady-state values with small fluctuations,[60] i.e., $a_1=a_{1\rm s}+\delta a_1$, $a_2=a_{2\rm s}+\delta a_2$, $b_1=b_{1\rm s}+\delta b_1$, $A=A_{\rm s}+\delta A$, $B_1=B_{1\rm s}+\delta B_1$, and $B_2=B_{2\rm s}+\delta B_2$. The steady-state values are considered to behave as

$$\begin{aligned}
a_{1\rm s} &= \frac{\varepsilon_{\rm c}}{(\kappa_1+{\rm i}\Delta_1)+\dfrac{J^2}{(\kappa_2+{\rm i}\bar{\Delta}_2)+\dfrac{G_B{}^2}{\gamma_{B_1}+{\rm i}\Delta_B+\dfrac{\Omega^2}{\gamma_{B_2}+{\rm i}E_{21}}}+\dfrac{G_A^2}{\gamma_A+{\rm i}\Delta_A}}},\\
a_{2\rm s} &= -\frac{{\rm i}Ja_{1\rm s}}{(\kappa_2+{\rm i}\bar{\Delta}_2)+\dfrac{G_B{}^2}{\gamma_{B_1}+{\rm i}\Delta_B+\dfrac{\Omega^2}{\gamma_{B_2}+{\rm i}E_{21}}}},\\
b_{1\rm s} &= -\frac{{\rm i}g|a_{2\rm s}|^2}{\gamma_{\rm m1}+{\rm i}\omega_{\rm m1}},\\
A_{\rm s} &= -\frac{{\rm i}G_A a_{1\rm s}}{\gamma_A+{\rm i}\Delta_A},\\
B_{1\rm s} &= -\frac{{\rm i}G_B a_{2\rm s}}{\gamma_{B_1}+{\rm i}\Delta_B+\dfrac{\Omega^2}{\gamma_{B_2}+{\rm i}E_{21}}},\\
B_{2\rm s} &= -\frac{{\rm i}\Omega B_{1\rm s}}{\gamma_{B_2}+{\rm i}E_{21}}.
\end{aligned}\tag{3}$$

The detuning has the form $\bar{\Delta}_2=\Delta_2+gx_{\rm s}$, in which $x_{\rm s}=b_{1\rm s}+b_{1\rm s}^{*}$. While we neglect the high-order small terms of the fluctuation parts during the operation, we can get the linearized quantum Langevin equations for the operators

$$\begin{aligned}
\delta\dot{a}_1 &= -(\kappa_1+{\rm i}\Delta_1)\delta a_1-{\rm i}J\delta a_2-{\rm i}G_A\delta A+\varepsilon_{\rm p}\,{\rm e}^{-{\rm i}\Delta_{\rm p}t},\\
\delta\dot{a}_2 &= -(\kappa_2+{\rm i}\bar{\Delta}_2)\delta a_2-{\rm i}J\delta a_1-{\rm i}G(\delta b_1^{\dagger}+\delta b_1)\\
&\quad-{\rm i}G_B\delta B_1,\\
\delta\dot{b}_1 &= -(\gamma_{\rm m1}+{\rm i}\omega_{\rm m1})\delta b_1-{\rm i}(G^{*}\delta a_2+G\delta a_2^{\dagger}),\\
\delta\dot{A} &= -(\gamma_A+{\rm i}\Delta_A)\delta A-{\rm i}G_A\delta a_1,\\
\delta\dot{B}_1 &= -(\gamma_{B_1}+{\rm i}\Delta_B)\delta B_1-{\rm i}G_B\delta a_2-{\rm i}\Omega\delta B_2,\\
\delta\dot{B}_2 &= -(\gamma_{B_2}+{\rm i}E_{21})\delta B_2-{\rm i}\Omega\delta B_1,
\end{aligned}\tag{4}$$

where $G=ga_{2\rm s}$. Assuming that the pump field is applied to drive the system at the mechanical red sideband with $\Delta_1=\bar{\Delta}_2=\omega_{\rm m1}=\Delta_A=\Delta_B=E_{21}=\omega_{\rm m}$, we make some transformations in the interaction picture, $\delta a_1\to\delta a_1\,{\rm e}^{-{\rm i}\Delta_{\rm p}t}$, $\delta a_2\to\delta a_2\,{\rm e}^{-{\rm i}\Delta_{\rm p}t}$, $\delta b_1\to\delta b_1\,{\rm e}^{-{\rm i}\Delta_{\rm p}t}$, $\delta A\to\delta A\,{\rm e}^{-{\rm i}\Delta_{\rm p}t}$, $\delta B_1\to\delta B_1\,{\rm e}^{-{\rm i}\Delta_{\rm p}t}$, and $\delta B_2\to\delta B_2\,{\rm e}^{-{\rm i}\Delta_{\rm p}t}$. After plugging them into Eq. (4), the steady state solution is equal to zero,[44,59,61] i.e., $\langle\delta\dot{a}_1\rangle=\langle\delta\dot{a}_2\rangle=\langle\delta\dot{b}_1\rangle=\langle\delta\dot{A}\rangle=\langle\delta\dot{B}_1\rangle=\langle\delta\dot{B}_2\rangle=0$, one can ignore the fast oscillating terms ${\rm e}^{2{\rm i}\Delta_{\rm p}t}$. We then get the following equation

$$\delta a_1=\frac{\varepsilon_{\rm p}}{\kappa_1+{\rm i}\delta+\dfrac{J^2}{\kappa_2+{\rm i}\delta+\dfrac{|G|^2}{\gamma_{\rm m1}+{\rm i}\delta}+\dfrac{G_B{}^2}{\gamma_{B_1}+{\rm i}\delta+\dfrac{\Omega^2}{\gamma_{B_2}+{\rm i}\delta}}+\dfrac{G_A^2}{\gamma_A+{\rm i}\delta}}},\tag{5}$$

where $\delta=\omega_{\rm m}-\Delta_{\rm p}$.

The response of the system can be derived by the input-output relation[62] as follows:

$$\varepsilon_{\rm out,p}=2\kappa_1\delta a_1-\varepsilon_{\rm p}.\tag{6}$$

We redefine the transmitted probe field as

$$\begin{aligned}
\varepsilon_{\rm T} &= \varepsilon_{\rm out,p}/\varepsilon_{\rm p}+1=2\kappa_1\delta a_1/\varepsilon_{\rm p}\\
&= \frac{2\kappa_1}{\kappa_1+{\rm i}\delta+\dfrac{J^2}{\kappa_2+{\rm i}\delta+\dfrac{|G|^2}{\gamma_{\rm m1}+{\rm i}\delta}+\dfrac{G_B{}^2}{\gamma_{B_1}+{\rm i}\delta+\dfrac{\Omega^2}{\gamma_{B_2}+{\rm i}\delta}}+\dfrac{G_A^2}{\gamma_A+{\rm i}\delta}}}.
\end{aligned}\tag{7}$$

3. Multiple-OMIT phenomena in the optomechanical system

In the following, we investigate the multiple-OMIT phenomena with interactions between the optical modes and two atomic ensembles. The experimental values are from

CPB Online In-Press

Ref. [63]. The relationships between the absorption and dispersion of the probe field with different coupling parameters and the effective detuning are shown in Fig. 2.

Figure 2(a) displays the absorption $\mathrm{Re}(\varepsilon_\mathrm{T})$ and the dispersion $\mathrm{Im}(\varepsilon_\mathrm{T})$ of the probe field as a function of δ/ω_m. Here all four coupling actions work. That is to say, not only are two atomic ensembles coupled into the cavities, but the two optical cavities are coupled to each other. Also, the mechanical oscillator b_1 interacts with the cavity a_2. The spectral lines of the probe field present five dips, which means the system becomes transparent to the probe field at five different frequencies.[44]

In Fig. 2(b), we consider the case where the coupling between the two-level atomic ensemble and the cavity field a_1 does not work, i.e., the effective coupling $G_A = 0$. It is found that the probe field has four transparency windows, i.e., four-OMIT. In other words, the two-level atomic ensemble contributes a transparency window to the optomechanical system. This is consistent with the result in Ref. [64].

Figure 2(c) shows the case that the three-level atomic ensemble has no coupling relationship with the optical mode a_2 ($G_B = 0$). Thus, three coupling effects left in the optomechanical system will act on the output response, which corresponds to the triple-OMIT. Note that the behavior of the output field can also be explained by the expression of ε_T, which changes significantly from Eq. (7). It has the expression as follows:

$$\varepsilon_\mathrm{T} = \frac{2\kappa_1}{\kappa_1 + \mathrm{i}\delta + \dfrac{J^2}{\kappa_2 + \mathrm{i}\delta + \dfrac{|G|^2}{\gamma_{\mathrm{m}1} + \mathrm{i}\delta} + \dfrac{G_A^2}{\gamma_A + \mathrm{i}\delta}}}, \tag{8}$$

corresponding to three transparency windows.

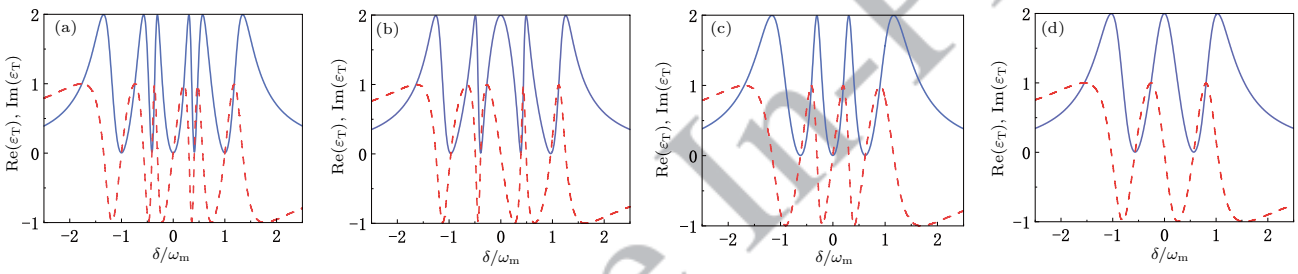


Fig. 2. Absorption and dispersion spectra of the probe field as a function of detuning δ/ω_m. (a) $G_A = 2\pi \times 8 \times 10^6$ Hz, $G_B = 2\pi \times 8 \times 10^6$ Hz; (b) $G_A = 0$, $G_B = 2\pi \times 8 \times 10^6$ Hz; (c) $G_A = 2\pi \times 8 \times 10^6$ Hz, $G_B = 0$; (d) $G_A = 0$, $G_B = 0$. For all plots, the system parameters are $m = 20$ ng, $\omega_\mathrm{m} = 2\pi \times 25 \times 10^6$ Hz, $Q = 6700$, $\gamma_{\mathrm{m}1} = \omega_\mathrm{m}/Q$, $\gamma_A = 2\pi \times 8 \times 10^3$ Hz, $\gamma_{B_1} = 2\pi \times 8 \times 10^3$ Hz, $\gamma_{B_2} = \gamma_{B_1}$, $\kappa_1 = 2\pi \times 14 \times 10^6$ Hz, $\kappa_2 = 2\pi \times 14 \times 10^3$ Hz, $P = 3 \times 10^{-3}$ W, $g = 2\pi \times 1.5 \times 10^3$ Hz, $J = 2\pi \times 12 \times 10^6$ Hz, $\Omega = 2\pi \times 8 \times 10^6$ Hz.

In Fig. 2(d), neither the two-level atomic ensemble nor the three-level atomic ensemble is considered in the system, i.e., $G_A = 0$ and $G_B = 0$. The phenomenon of induced transparency comes from the two optical modes and the mechanical mode. The output field behavior of the hybrid system exhibits two transparency windows. Here, ε_T is changed to

$$\varepsilon_\mathrm{T} = \frac{2\kappa_1}{\kappa_1 + \mathrm{i}\delta + \dfrac{J^2}{\kappa_2 + \mathrm{i}\delta + \dfrac{|G|^2}{\gamma_{\mathrm{m}1} + \mathrm{i}\delta}}}, \tag{9}$$

which is a standard form for the double-OMIT.[54]

The multiple-OMIT can be understood by the quantum interference paths between different energy levels within the hybrid cavity optomechanical system as shown in Fig. 3. When the coupling effect between the two-level atomic ensemble and the cavity field a_1 disappears, i.e., $G_A = 0$, the number of transparency windows will decrease by one as the interference path decreases. This is the four-OMIT. If $G_B = 0$ and $G_A \neq 0$, although the two-level atomic ensemble coupling still exists, the interference path between the three-level atomic ensemble and the cavity field a_2 is blocked. So the output field behaves as triple-OMIT. Furthermore, when the coupling effects between the atomic ensembles and the cavity fields disappear, the quantum interference path only exists between the cavity field a_1 and cavity field a_2, and between the cavity field a_2 and the mechanical resonator b_1. Then the output field manifests itself as the double-OMIT.

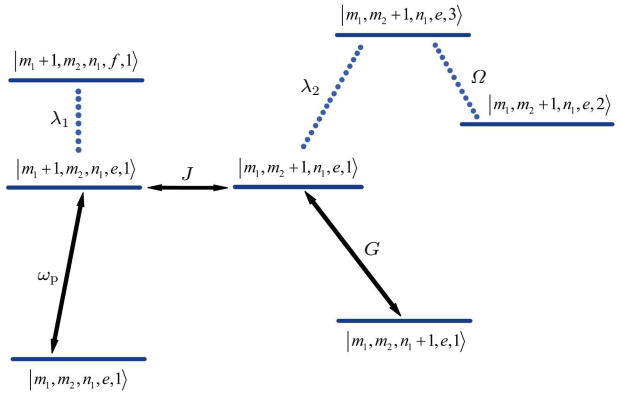


Fig. 3. Energy-level diagram of the system with $\omega_{b_1} = \omega_\mathrm{m}$. $|m_1\rangle$, $|m_2\rangle$, and $|n_1\rangle$ denote the number states of two cavity modes and mechanical mode, respectively.

4. Coupling effects on the multiple-OMIT

Now we turn to explore the characteristics of the OMIT arising from the interactions of the internal components within the system. The absorption $\mathrm{Re}(\varepsilon_\mathrm{T})$ as a function of δ/ω_m for four different coupling effects demonstrates the influence of changing coupling strength on the behavior of the probe field.

Figure 4(a) shows the simulation of the coupling effect between the optical mode and the mechanical mode on the

CPB Online In Press

OMIT. For a coupling parameter of $g = 0$, it can be clearly seen that the OMIT behaves as three transparency windows. As the coupling appears, the transparency window in the middle splits and evolves into three transparency windows.[55] However, if the coupling strength increases to $g = 2\pi \times 15 \times 10^3$ Hz, there is only one single transparency window left in the system.

In Fig. 4(b), the absorption $\mathrm{Re}(\varepsilon_{\mathrm{T}})$ is associated with the coupling coefficient J between the two cavity fields. It is easy to find that the system will add four new transparency windows if the first cavity is coupled with the second cavity. The variation of width in the transparency window is mainly induced by the J, i.e., the distance of the outermost transparency windows will widen with the increase of J.

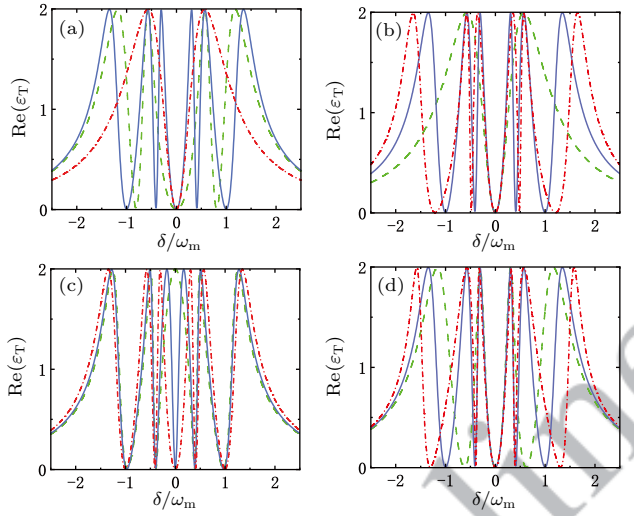


Fig. 4. Absorption spectra $\mathrm{Re}(\varepsilon_{\mathrm{T}})$ as functions of $\delta/\omega_{\mathrm{m}}$. (a) $g = 0$ (dashed line), $g = 2\pi \times 1.5 \times 10^3$ Hz (solid line) and $g = 2\pi \times 15 \times 10^3$ Hz (dashed-dotted line). (b) $J = 0$ (dashed line), $J = 2\pi \times 12 \times 10^6$ Hz (solid line) and $J = 2\pi \times 15 \times 10^6$ Hz (dashed-dotted line). (c) $G_A = 0$ (dashed line), $G_A = 2\pi \times 4 \times 10^6$ Hz (solid line) and $G_A = 2\pi \times 8 \times 10^6$ Hz (dashed-dotted line). (d) $G_B = 0$ (dashed line), $G_B = 2\pi \times 8 \times 10^6$ Hz (solid line) and $G_B = 2\pi \times 12 \times 10^6$ Hz (dashed-dotted line). Other parameters are the same as those in Fig. 2.

Figure 4(c) demonstrates the coupling effect G_A of the two-level atomic ensemble on the absorption of the probe field. When $G_A = 0$, the behavior of the probe field is four-OMIT. When the two-level atomic ensemble is coupled to the optical mode, the single transparency window in the middle splits into two, which leads to the occurrence of five-OMIT. Moreover, the change of G_A also results in the small movement of the transparent points.

Figure 4(d) presents the variation of the absorption $\mathrm{Re}(\varepsilon_{\mathrm{T}})$ for different G_B values between the three-level atomic ensemble and the optical mode a_2. Remarkably, the transparency windows in the probe field are split from three to five owing to the coupling relationship being established. In other words, the three-level atomic ensemble contributes two transparency windows, which has also been proved in Ref. [54]. The width of the outermost transparency windows can be expanded by increasing G_B, and the corresponding transparent points will also move further away.

5. Fast/slow light of the probe field

To investigate the slow/fast effect, we consider the dependence of the phase and group delay on the frequency detuning $\delta/\omega_{\mathrm{m}}$. The transmission of the probe field is related to the frequency of the output field and the frequency of the input field, which has the following form:

$$t_{\mathrm{p}}(\omega_{\mathrm{p}}) = \frac{\varepsilon_{\mathrm{p}} - 2\kappa_1 \delta a_1}{\varepsilon_{\mathrm{p}}} = 1 - \frac{2\kappa_1 \delta a_1}{\varepsilon_{\mathrm{p}}}. \tag{10}$$

The action of the external control field results in a rapid phase dispersion $\phi_t(\omega_{\mathrm{p}}) = \arg\left[t_{\mathrm{p}}(\omega_{\mathrm{p}})\right]$, which is associated with the group delay of the transmission[65–67]

$$\tau = \frac{\mathrm{d}\phi_t(\omega_{\mathrm{p}})}{\mathrm{d}\omega_{\mathrm{p}}} = \frac{\mathrm{d}\left\{\arg\left[t_{\mathrm{p}}(\omega_{\mathrm{p}})\right]\right\}}{\mathrm{d}\omega_{\mathrm{p}}}. \tag{11}$$

By tuning the phase, we can change the value of τ. A positive (negative) group delay $\tau > 0$ ($\tau < 0$) corresponds to slow (fast) light propagation.[63,68] As shown in Figs. 5(a) and 5(b), the phase ϕ_t and the group delay τ of the probe field are plotted as a function of the detuning $\delta/\omega_{\mathrm{m}}$, respectively. Figure 5(a) shows that the spectrum of the phase can be changed by manipulating the detuning. The five steep changes correspond to the five group delays. In Fig. 5(b), there are two parts where the group delay $\tau > 0$, meaning that the system exhibits slow light phenomena. The fast light phenomena correspond to the points where the group delays are negative ($\tau < 0$). Thus, we can transform the probe field from slow light to fast light by controlling detuning.

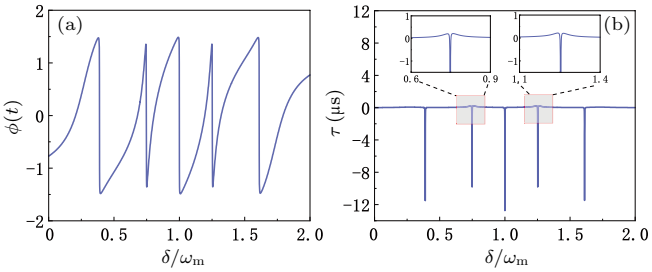


Fig. 5. (a) Phase of the probe field as a function of the normalized frequency $\delta/\omega_{\mathrm{m}}$. (b) Group velocity delay τ as a function of the normalized frequency $\delta/\omega_{\mathrm{m}}$. The parameters used for the simulation are the same as those in Fig. 2.

6. Conclusion

We investigate the optical response of the probe field in the two-cavity optomechanical system containing both the two-level and three-level atomic ensembles. The relationship between the characteristics of transparency windows and system parameters is explored. Generally, the system exhibits five transparency windows in the probe field spectrum. The absence of the two-level atomic ensemble induces four transparency windows. Furthermore, removing the three-level atomic ensemble, the number of transparency windows will be reduced to three. The output field spectrum behaves as two

CPB Online In Press

transparency windows when the hybrid system contains only two optical cavities and one mechanical resonator. We also demonstrate that the width of the transparency windows can be broadened as the coupling strength increases and transform the probe field from slow light to fast light by adjusting the detuning. These results are beneficial to the study of nonlinear optical effects and promising applications such as the manipulation of optoelectronic devices.

Data availability statement

Data are available from the corresponding authors upon reasonable request.

Acknowledgements

This work was partially supported by the Quantum Science and Technology-National Science and Technology Major Project (Grant No. 2021ZD0301701), State Key Laboratory for Novel Software Technology at Nanjing University, Dengfeng Project of Nanjing University, and Ministry of Education Engineering Research Center for Optoelectronic Materials and Chip Technology.

References

[1] Arregui G, Ng R C, Albrechtsen M, Stobbe S, Sotomayor-Torres C M and García P D 2023 *Phys. Rev. Lett.* **130** 043802
[2] Laha P, Ameen Yasir P A and Loock P V 2024 *Phys. Rev. Research* **6** 033302
[3] Jiang C, Song L N and Li Y 2018 *Phys. Rev. A* **97** 053812
[4] Alinaghipour R and Mohammadi H 2024 *Phys. Rev. A* **110** 032412
[5] Kharel P, Chu Y, Mason D, Kittlaus E A, Otterstrom N T, Gertler S and Rakich P T 2022 *Phys. Rev. Appl.* **18** 024054
[6] Tang J and Deng Y 2024 *Phys. Rev. Research* **6** 033247
[7] Sesin P, Anguiano S, Bruchhausen A E, Lemaître A and Fainstein A 2021 *Phys. Rev. B* **103** 081301
[8] Zhou B Y, Pan N, Yu L and Li G X 2024 *Phys. Rev. A* **110** 032401
[9] Wu Y, Nie W J, Li G Y, Chen A X and Lan Y H 2021 *Phys. Rev. A* **103** 043521
[10] Singh S K and Ooi C H R 2014 *J. Opt. Soc. Am. B* **31** 2390
[11] Singh S K, Mazaheri M, Peng J X, Sohail A, Khalid M and Asjad M 2023 *Front. Phys.* **11** 1142452
[12] Zhang J L, Orszag M, Xiao M, Jiang X S, Lin Q and He B 2024 *Phys. Rev. Lett.* **133** 103602
[13] Singh S K, Mazaheri M, Peng J X, Sohail A, Gu Z and Asjad M 2023 *Quantum Inf. Process.* **22** 198
[14] Wang J, Zhang Q and Jing H 2024 *Phys. Rev. A* **110** 033505
[15] Singh S K, Parvez M, Abbas T, Peng J X, Mazaheri M and Asjad M 2022 *Phys. Lett. A* **442** 128181
[16] Singh S K, Peng J X, Asjad M and Mazaheri M 2021 *J. Phys. B: At. Mol. Opt. Phys.* **54** 215502
[17] Singh S K, Asjad M and Raymond Ooi C H 2022 *Quantum Inf. Process.* **21** 47
[18] Amazioug M, Daoud M, Singh S K and Asjad M 2023 *Quantum Inf. Process.* **22** 301
[19] Singh S K and Muniandy S V 2016 *Int. J. Theor. Phys.* **55** 287
[20] Kundu A and Singh S K 2019 *Int. J. Theor. Phys.* **58** 2418
[21] Yusoff F N, Zulkifli M A, Ali N, Singh S K, Abdullah N, Hambali N and Edet C O 2023 *Photonics* **10** 279
[22] Hidki A, Peng J X, Singh S K, Khalid M and Asjad M 2024 *Sci. Rep.* **14** 11204
[23] Wollman E E, Lei C U, Weinstein A J, Suh J, Kronwald A, Marquardt F, Clerk A A and Schwab K C 2015 *Science* **349** 952
[24] Safavi-Naeini A H, Mayer Alegre T P, Chan J, Eichenfield M, Winger M, Lin Q, Hill J T, Chang D E and Painter O 2011 *Nature* **472** 69
[25] Lü X Y, Zhang W M, Ashhab S, Wu Y and Nori F 2013 *Sci. Rep.* **3** 2943
[26] Huang S M and Agarwal G S 2009 *Phys. Rev. A* **80** 033807
[27] Massel F, Heikkilä T T, Pirkkalainen J M, Cho S U, Saloniemi H, Hakonen P J and Sillanpää M A 2011 *Nature* **480** 351
[28] He Y 2015 *Phys. Rev. A* **91** 013827
[29] Koppenhöfer M, Padgett C, Cady J V, Dharod V, Oh H, Jayich A and Clerk A A 2023 *Phys. Rev. Lett.* **130** 093603
[30] Agarwal G S and Huang S M 2012 *Phys. Rev. A* **85** 021801(R)
[31] Willner A E, Zhang B, Zhang L, Yan L and Fazal I 2008 *IEEE J. Sel. Top. Quantum Electron.* **14** 691
[32] Liu Y C, Xiao Y F, Luan X S, Gong Q H and Wong C W 2015 *Phys. Rev. A* **91** 033818
[33] He L, Liu Y X, Yi S, Sun C P and Nori F 2007 *Phys. Rev. A* **75** 063818
[34] Zhang J Q, Li Y, Feng M and Xu Y 2012 *Phys. Rev. A* **86** 053806
[35] Jiang C, Cui Y S, Bian X T, Zuo F, Yu H L and Chen G B 2016 *Phys. Rev. A* **94** 023837
[36] Zhang X Y, Zhou Y H, Guo Y Q and Yi X X 2018 *Phys. Rev. A* **98** 033832
[37] Lu T X, Jiao Y F, Zhang H L, Saif F and Jing H 2019 *Phys. Rev. A* **100** 013813
[38] Lai D G, Wang X, Qin W, Hou B P, Nori F and Liao J Q 2020 *Phys. Rev. A* **102** 023707
[39] Sütlüoğlu B and Bulutay C 2021 *Phys. Rev. A* **104** 033504
[40] Shahidani S, Naderi M H and Soltanolkotabi M 2013 *Phys. Rev. A* **88** 053813
[41] Man X X, Sun J, Zhang W Z, Luo L J and Jin G R 2024 *Chin. Phys. B* **33** 120303
[42] Chen L T, Qin L G, Tian L J, Huang J H, Zhou N R and Gong S Q 2024 *Chin. Phys. B* **33** 064204
[43] Xiao R J, Pan G X and Zhou L 2015 *J. Opt. Soc. Am. B* **32** 1399
[44] Ma J L, Tan L, Li Q, Gu H Q and Liu W M 2018 *Sci. Rep.* **8** 14367
[45] Wu S C, Qin L G, Jing J, Yang G H and Wang Z Y 2016 *Chin. Phys. B* **25** 054203
[46] Ullah K, Jing H and Saif F 2018 *Phys. Rev. A* **97** 033812
[47] Chang Y, Shi T, Liu Y X, Sun C P and Nori F 2011 *Phys. Rev. A* **83** 063826
[48] Di K, Xia H R, Diao W T, Cai C X, Yang W H, Qin Y L, Liao Z T, He Y C and Du J J 2025 *Chin. Phys. B* **34** 074201
[49] Li J, Zhou M T, Yang C W, Sun P F, Liu J L, Bao X H and Pan J W 2019 *Phys. Rev. Lett.* **123** 140504
[50] Zhou C, Maleki Y, Liao Z and Zubairy M S 2023 *Phys. Rev. A* **108** 013708
[51] Chen W Y and Milburn G J 1997 *Phys. Rev. E* **56** 351
[52] Hotter C, Ostermann L and Ritsch H 2023 *Phys. Rev. Research* **5** 013056
[53] Schleier-Smith M H, Leroux I D, Zhang H, Van Camp M A and Vuletić V 2011 *Phys. Rev. Lett.* **107** 143005
[54] Xiao R J, Pan G X, Xiu X M and Liu Y 2020 *Laser Phys. Lett.* **17** 105206
[55] Hao H, Kuzyk M C, Ren J, Zhang F, Duan X, Zhou L, Zhang T, Gong Q, Wang H and Gu Y 2019 *Phys. Rev. A* **100** 023820
[56] Guo Y, Li K, Nie W and Li Y 2014 *Phys. Rev. A* **90** 053841
[57] Xu X W and Li Y 2014 *Phys. Rev. A* **90** 033809
[58] Yu C, Guan X, Yang W, Chen F and Wang B 2024 *Opt. Quantum Electron.* **56** 41
[59] Jia W Z, Wei L F, Li Y and Liu Y X 2015 *Phys. Rev. A* **91** 043843
[60] Aspelmeyer M, Kippenberg T J and Marquardt F 2014 *Rev. Mod. Phys.* **86** 1391
[61] Jiang C, Jiang L, Yu H, Cui Y, Li X and Chen G 2017 *Phys. Rev. A* **96** 053821
[62] Walls D F and Milburn G J 1994 *Quantum Optics* pp. 315–340
[63] Weis S, Rivière R, Deléglise S, Gavartin E, Arcizet O, Schliesser A and Kippenberg T J 2010 *Science* **330** 1520
[64] Pan G X, Xiao R J, Chen H J and Gao J 2021 *Laser Phys.* **31** 065202
[65] Walls D F and Milburn G J 1994 *Quantum Optics* pp. 279–314
[66] Tarhan D, Huang S M and Müstecaplioğlu Ö E 2013 *Phys. Rev. A* **87** 013824
[67] Wu Z, Luo R H, Zhang J Q, Wang Y H, Yang W and Feng M 2017 *Phys. Rev. A* **96** 033832
[68] Zhan X G, Si L G, Zheng A S and Yang X 2013 *J. Phys. B: At. Mol. Opt. Phys.* **46** 025501

Online In Press